Perrella, M., Heyda, A., Mosca, A., & Rossi-Bernardi, L. (1978) *Anal. Biochem. 88*, 212-224.
Perrella, M., Cremonesi, L., Benazzi, L., & Rossi-Bernardi, L. (1981) *J. Biol. Chem. 256*, 11098-11103.
Perrella, M., Benazzi, L., Cremonesi, L., Vesely, S., Viggiano, G., & Berger, R. L. (1983) *J. Biochem. Biophys. Methods 7*, 187-197.
Pettigrew, D. W., Romeo, P. H., Tsapis, A., Thillet, J., Smith, M. L., Turner, B. W., & Ackers, G. K. (1982) *Proc. Natl. Acad. Sci. U.S.A. 79*, 1849-1853.
Sack, J., Andrew, L., Magnus, K., Hanson, J., Rubin, J., & Love, W. (1978) *Hemoglobin 2*, 153-169.
Schroeder, W. A., & Huisman, T. H. J. (1980) *The Chromatography of Hemoglobin*, Marcel Dekker, New York.
Smith, F. R. (1985) Ph.D. Dissertation, The Johns Hopkins University.
Smith, F. R., & Ackers, G. K. (1985) *Proc. Natl. Acad. Sci. U.S.A. 82*, 5347-5351.
Turner, B. W., Pettigrew, D. W., & Ackers, G. K. (1981) *Methods Enzymol. 76*, 596-628.
Turner, G. J. (1989) Ph.D. Dissertation, The Johns Hopkins University.
Williams, R. C., & Tsay, K. (1973) *Anal. Biochem. 54*, 137-145.

Alteration of Sperm Whale Myoglobin Heme Axial Ligation by Site-Directed Mutagenesis†

Karen D. Egeberg,‡ Barry A. Springer,‡ Susan A. Martinis, and Stephen G. Sligar*
Departments of Biochemistry and Chemistry, University of Illinois, Urbana, Illinois 61801
Dimitrios Morikis§ and Paul M. Champion*
Department of Physics, Northeastern University, Boston, Massachusetts 02115
Received November 15, 1989; Revised Manuscript Received July 16, 1990

ABSTRACT: Three mutant proteins of sperm whale myoglobin (Mb) that exhibit altered axial ligations were constructed by site-directed mutagenesis of a synthetic gene for sperm whale myoglobin. Substitution of distal pocket residues, histidine E7 and valine E11, with tyrosine and glutamic acid generated His(E7)Tyr Mb and Val(E11)Glu Mb. The normal axial ligand residue, histidine F8, was also replaced with tyrosine, resulting in His(F8)Tyr Mb. These proteins are analogous in their substitutions to the naturally occurring hemoglobin M mutants (HbM). Tyrosine coordination to the ferric heme iron of His(E7)Tyr Mb and His(F8)Tyr Mb is suggested by optical absorption and EPR spectra and is verified by similarities to resonance Raman spectral bands assigned for iron–tyrosine proteins. His(E7)Tyr Mb is high-spin, six-coordinate with the ferric heme iron coordinated to the distal tyrosine and the proximal histidine, resembling Hb M Saskatoon [His(βE7)Tyr], while the ferrous iron of this Mb mutant is high-spin, five-coordinate with ligation provided by the proximal histidine. His(F8)Tyr Mb is high-spin, five-coordinate in both the oxidized and reduced states, with the ferric heme iron liganded to the proximal tyrosine, resembling Hb M Iwate [His(αF8)Tyr] and Hb M Hyde Park [His(βF8)Tyr]. Val(E11)Glu Mb is high-spin, six-coordinate with the ferric heme iron liganded to the F8 histidine. Glutamate coordination to the ferric iron of this mutant is strongly suggested by the optical and EPR spectral features, which are consistent with those observed for Hb M Milwaukee [Val(βE11)Glu]. The ferrous iron of Val(E11)Glu Mb exhibits a five-coordinate structure with the F8 histidine–iron bond intact. The results presented here demonstrate the power of site-directed mutagenesis as a tool for altering the electronic structure of metal centers and aiding in the assignment of complicated vibrational spectra.

Heme proteins are ubiquitous, assuming varied roles in biochemistry. Typically, they are classified on the basis of their ligation to the iron center. Four of the six heme iron coordinate positions are occupied by protoporphyrin IX pyrrole nitrogens with one or both of the two remaining coordinate positions occupied by the protein moiety. Six-coordinate electron-transfer proteins include bis-imidazole-ligated *b*-type cytochromes and the methionine–histidine coordination of *c*-type cytochromes. Heme proteins with an open coordination site include the oxygen storage and transport proteins (myoglobin and hemoglobin) and peroxidases with histidine ligation, catalases with tyrosine ligation, and cytochromes P-450 and chloroperoxidase with cysteine as the fifth axial ligand. The iron–imidazole bond in myoglobin (Mb) and hemoglobin (Hb) and its effect on the iron–porphyrin out of plane displacement (Srajer et al., 1988) are thought to have a major role in the mechanisms which control ligand affinity and the transition of the R to T state in Hb [Perutz (1970, 1987) and references cited therein].

The construction of a synthetic gene for sperm whale Mb and the resultant high-level expression of this gene as heme-containing protein in *Escherichia coli* (Springer & Sligar, 1987) have enabled us to genetically engineer sperm whale Mb by in vitro mutagenesis techniques. Substitution of the proximal histidine (F8) with a tyrosine, His(F8)Tyr,[1] the distal

† This work was supported by NIH GM33775 and NIH GM31756 (S.G.S.) and NIH AM35090 and NSF DMB8716382 (P.M.C.).
* To whom correspondence should be addressed.
‡ Present address: Department of Chemistry, University of California, Berkeley, CA 94720.
§ Present address: Department of Molecular Biology, Research Institute of Scripps Clinic, La Jolla, CA 92037.

0006-2960/90/0429-9783$02.50/0

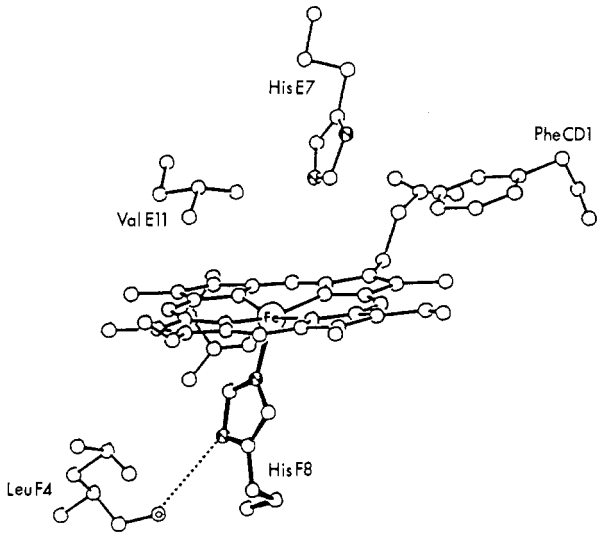

FIGURE 1: Ball and stick figure of the active site residues His E7, Val E11, and Phe CD1 (Stayton et al., 1989). Also included is the proximal histidine (His F8) bound to the heme iron. The His E7, Val E11, and His F8 residues are the subject of site-directed mutagenesis efforts designed to alter the myoglobin heme iron axial ligation.

histidine (E7) with a tyrosine, His(E7)Tyr, and the distal valine (E11) with a glutamate, Val(E11)Glu, resulted in proteins with altered heme–iron ligations. The active site residues of sperm whale Mb, analogous to those found in α and β subunits of normal human Hb, can be seen in Figure 1. These myoglobin mutants are analogous in their substitutions to Hbs M, a class of natural Hb mutants in which the α or β subunit is stabilized in the ferric form physiologically, and therefore unable to bind O_2. In these Hb mutants, which include Hb M Boston [His(αE7)Tyr], Hb M Saskatoon [His(βE7)Tyr], Hb M Iwate [His(αF8)Tyr], Hb M Hyde Park [His(βF8)Tyr], and Hb M Milwaukee [Val(βE11)Glu], the phenolate group of tyrosine or the carboxylate group of glutamic acid is coordinated to the heme iron in the abnormal subunit, as determined by X-ray structural data (Greer, 1971; Perutz et al., 1972; Pulsinelli et al., 1973). The spectral characteristics of these mutants also have been probed by resonance Raman spectroscopy (Nagai et al., 1983, 1989). In addition, Boxer and co-workers constructed a mutant of human Mb in which the valine E11 residue was replaced by glutamic acid. Characterization of this mutant by circular dichroism, optical absorption, and NMR spectroscopies revealed a ligation state similar to that observed for Hb M Milwaukee (Varadarajan et al., 1989a,b). In this paper we have characterized three sperm whale Mb mutant proteins by optical, electron paramagnetic resonance, and resonance Raman spectroscopies and have examined the arrangement of the axial ligands of these mutants in their various oxidation states.

Experimental Procedures

Mutagenesis. The design and construction of the synthetic myoglobin gene pMb413 are described by Springer and Sligar (1987). Cassette mutagenesis was utilized to construct the following mutants: For the construction of His(E7)Tyr Mb and Val(E11)Glu Mb, the vector pMb413 was digested with the restriction enzymes *Bgl*II and *Hpa*I. A set of mixed oligonucleotides constituting both strands of DNA included the replacement of the distal His codon (CAT) with TAT (Tyr). Another mixed set of oligonucleotides replaced the ValE11 codon (GTG) with GAA (Glu). The oligonucleotides were annealed and ligated at a 10-fold molar excess with the *Bgl*II–*Hpa*I-digested vector. In these constructions, the *Hpa*I site was eliminated for convenient screening. For the construction of His(F8)Tyr Mb, pMb413 was recloned into a pUC vector with a modified polylinker region. This new Mb clone, designated pMb413a, was digested with *Sph*I, leaving a 3′-overhang. T4 DNA polymerase (3′-exonuclease activity) was used to generate a blunt end, and the vector was then digested with *Eco*RI. Two mixed oligonucleotides were inserted into position 214 to the *Eco*RI site of the digested vector at a 10-fold molar excess, thus replacing the normal proximal His codon (CAT) with TAT (Tyr).

All DNA manipulations were performed essentially as described by Maniatis et al. (1982), with double-stranded DNA sequencing performed as described by Hattori and Sakaki (1986). All enzymes used in this study were purchased from Bethesda Research Laboratories with the exception of T4 DNA polynucleotide kinase, which was purchased from New England BioLabs. Oligonucleotides were synthesized by the University of Illinois (Urbana–Champaign) Biotechnology Center and purified by reverse-phase HPLC as described by Springer and Sligar (1987). All mutant constructions were expressed in *E. coli* strain TB-1 [*ara*, Δ(*lac-pro*), *strA*, *thi*, Φ*80dlacZ*Δ*M15*, r^-, m^+; T. O. Baldwin, Texas A&M University, College Station, TX].

Protein Purification. The His(E7)Tyr Mb and Val(E11)Glu Mb proteins were purified as previously described (Springer & Sligar, 1987). These proteins were overexpressed in *E. coli* as heme-containing Mb to approximately 10% of the total soluble protein, resulting in a dark brown cell paste as is seen with wild-type Mb. During purification these protein preparations turned greenish and remained stable as such. These Mb mutant proteins were determined to be >90% pure by SDS–polyacrylamide gel electrophoresis.

His(F8)Tyr Mb was expressed in *E. coli* to a high level predominantly as apoprotein (<10% heme incorporated). A purification scheme similar to that of the heme-containing Mb mutants was used for this apo-His(F8)Tyr Mb protein. The apoprotein was then reconstituted with hemin chloride at a protein:hemin ratio of 1:2 in 0.1 M potassium phosphate (pH 9.0), 0.1 M potassium chloride, and 10% glycerol. After several hours at 4 °C, the reconstituted sample was passed over a Sephadex G-25 column (preequilibrated in 0.1 M potassium phosphate, pH 9.0, 1 mM EDTA) to remove excess hemin. The protein was then concentrated and the buffer exchanged with 0.1 M potassium phosphate, pH 9.0.

Spectroscopy. Optical spectra of purified proteins in 0.1 M potassium phosphate, pH 7.0, were recorded on Hewlett-Packard 8450A, Perkin-Elmer 320, or Varian 219 UV/visible spectrophotometers. Electron paramagnetic resonance (EPR) spectroscopy was performed on wild-type and mutant Mbs on a Bruker EPR200 D-SRC [modulation frequency, 100 kHz; modulation amplitude, 10 G; power, 16 dB (5 mW) at 7.3 K] equipped with a Bruker microwave bridge ERO4MRH, helium Dewar, Varian gauss meter, and EIP microwave 548A frequency meter. Typical protein concentrations were 300 μM protein in 0.1 M potassium phosphate (pH 7.0) for wild-type Mb, His(E7)Tyr Mb, and Val(E11)Glu Mb and 300 μM protein in 0.1 M potassium phosphate (pH 9.0) for His(F8)Tyr Mb. The His(F8)Tyr Mb mutant was most stably reconstituted in 0.1 M potassium phosphate (pH 9.0) and generated

[1] Myoglobin mutants and hemoglobin variants are indicated by the wild-type amino acid and mutant residue separated by the position in parentheses. Hence, His(F8)Tyr is the replacement of histidine by tyrosine at the F8 position, the eighth residue of the F-helix, following the standard globin nomenclature (Dickerson & Geis, 1983).

the cleanest EPR and resonance Raman spectra under these buffer conditions. Data manipulation was achieved on an IBM PC using in-house software (Morse, 1987). EPR experiments were carried out at the University of Illinois (Urbana–Champaign) EPR Center.

Room-temperature resonance Raman spectra were taken of Mb samples with excitation wavelengths at 416 and 488 nm for ferric forms, at 430 nm for the ferrous (deoxy) forms, and at 420 nm for the carbon monoxy adducts. Typical protein concentrations were 30–60 μM for Soret excitation and 300–900 μM for 488-nm excitations in the buffers indicated: Val(E11)Glu Mb [20 mM Tris-HCl (pH 8.4), 1 mM EDTA], His(F8)Tyr Mb [0.1 M potassium phosphate (pH 9.0)], and His(E7)Tyr Mb and native sperm whale Mb [0.1 M potassium phosphate (pH 7.0)]. Raman spectra were taken with instrumentation previously described (Morikis et al., 1989). All samples were checked before and after the Raman experiments with a high-resolution Perkin-Elmer 320 UV/visible absorption spectrophotometer.

Results

The use of site-directed mutagenesis to assess the role of axial ligands in heme protein function has proved difficult as a result of the evident importance of the native axial ligand(s) in normal protein folding, thus leading to the production of holoproteins. In all known cases of heme protein axial ligand site-directed mutagenesis, the proteins have been expressed in bacterial hosts as apoproteins. This includes the His(F8)Tyr mutant of Mb presented in this paper, the His(39)Met mutant of cytochrome b_5 (Sligar et al., 1987), and axial ligand mutants of cytochrome P-450$_{cam}$ (Unger, 1988) and rat liver cytochrome P-450 (Shimizu et al., 1988).

UV–Visible Spectroscopy. Optical absorption spectra of Fe^{3+} (oxidized), Fe^{2+} (reduced), $Fe^{2+}O_2$ (MbO_2), and $Fe^{2+}CO$ (MbCO) forms of wild-type and mutant Mbs are summarized in Table I. Charge-transfer bands at ca. 485 and 600 nm seen for His(E7)Tyr Mb and His(F8)Tyr Mb, characteristic of high-spin ferric heme, are also seen in Hb M Boston [His(αE7)Tyr], Hb M Saskatoon [His(βE7)Tyr], Hb M Iwate [His(αF8)Tyr], and Hb M Hyde Park [His(βF8)Tyr] (Nagai et al., 1983, 1989). Similar absorption bands in the 470–490-nm range have been observed in the non heme iron–phenolate proteins and model compounds (Que, 1988) and have been assigned to phenolate–Fe(III) p_π–d_{π^*} charge-transfer bands (Gaber et al., 1974). Bands at ca. 495 and 620 nm for Val(E11)Glu Mb are also observed in Hb M Milwaukee [Val(βE11)Glu] (Hayashi et al., 1969) and human Mb Val(E11)Glu (Varadarajan et al., 1989b). Slight shifts in the Soret were observed for the oxidized forms of His(E7)Tyr Mb, His(F8)Tyr Mb, and Val(E11)Glu Mb, whereas the His(F8)Tyr Mb exhibited a shift in the Soret of the deoxy spectrum. His(E7)Tyr Mb did not form a stable MbO_2 complex due to rapid heme iron oxidation. His(F8)Tyr Mb and Val(E11)Glu Mb also autoxidized rapidly compared to wild-type Mb; therefore, temperatures of 4 °C were required to determine an approximate Soret for the MbO_2 complex (Table I). In contrast, all mutant myoglobin proteins exhibited stable CO complexes at room temperature.

Electron Paramagnetic Resonance Spectroscopy. Figure 2 presents the electron paramagnetic resonance (EPR) spectra at 7.3 K of wild-type and mutant Mbs with tyrosine replacement at positions F8 and E7 and glutamate substitution at position E11. The spectra of these mutant Mbs indicate high-spin proteins with rhombically split signals in the $g = 6$ region. His(F8)Tyr Mb exhibited multiple g values of 6.85, 6.25, 6.08, 4.72, 2.04, and 1.99, suggestive of at least two

Table I: Optical Spectral Properties of Mutant and Wild-Type Synthetic Sperm Whale Mb and Human Hb[a]

	Fe^{3+}				
			visible		
protein	δ	Soret			CT
His(E7)Tyr Mb	350	410	486	542	600
His(F8)Tyr Mb	350	402	480	524	598
Val(E11)Glu Mb	350	406	496	536	618
wild-type Mb		408	502		632

	Fe^{2+}	
protein	Soret	visible
His(E7)Tyr Mb	432	558
His(F8)Tyr Mb	428	556
Val(E11)Glu Mb	434	560
wild-type Mb	432	554

	$Fe^{2+}O_2$			
		visible		
protein	Soret	β	α	
His(E7)Tyr Mb[b]				
His(F8)Tyr Mb	~414	540	576	
Val(E11)Glu Mb	~410	540	580	626
wild-type Mb	418	544	580	626

	$Fe^{2+}CO$		
		visible	
protein	Soret	β	α
His(E7)Tyr Mb	424	542	574
His(F8)Tyr Mb	418	536	568
Val(E11)Glu Mb	420	540	578
wild-type Mb	422	542	578

	visible for Fe^{3+} form			
protein		β	α	CT
met-Hb A	500	540	570	630
Hb M Boston	490			600
Hb M Saskatoon	485			600
Hb M Iwate	480			590
Hb M Hyde Park	490			580
Hb M Milwaukee	495	535	575	620

[a] Optical spectra properties of Hb M mutants and Hb A from Nagai et al. (1983, 1989) and Nagai and Yoneyama (1983). [b] His(E7)Tyr Mb oxidized too rapidly to obtain an $Fe^{2+}O_2$ species.

ligation states. Although the identity of the signal is typically indicated by the cross peak, the trough with a g value of 4.72 is marked because of the complicated spectrum of this mutant (Figure 2C). These results contrast the reported g values of the analogous Hb mutants: Hb M Iwate, $g = 6.2$ and 5.8; Hb M Hyde Park, $g = 6.31$, 5.68, and 2.0 (Hayashi et al., 1969). His(E7)Tyr Mb exhibited g values of 6.63, 5.31, and 1.98, which are similar to those reported for Hb M Saskatoon, $g = 6.65$, 6.0, 5.35, 4.3, and 2.0 (Hayashi et al., 1969). Another analogous Hb mutant, Hb M Boston, differs from His(E7)Tyr Mb with g values of 6.3, 5.71, and 2.0 (Hayashi et al., 1969). Val(E11)Glu Mb shows an axial and rhombic component with g values of 6.76, 6.0, 5.2, and 1.97, which are comparable to those of Hb M Milwaukee [Val(βE11)Glu], $g = 6.86$, 6.05, 5.05, and 1.95. In Table II, which is modified from Palmer (1979), are displayed several native heme proteins, natural Hb mutants, and sperm whale Mb mutants with their precent rhombicity, as defined by Peisach et al. (1971). High rhombicity is exhibited for His(E7)Tyr Mb, as seen with both bovine catalase, a tyrosine-liganded heme protein, and Hb M Saskatoon. In addition, the Val(E11)Glu Mb also displays high rhombicity, nearly identical with that reported for Hb M Milwaukee. The His(F8)Tyr Mb mutant does not resemble either of its analogous Hb mutants, M Iwate or M Hyde Park, which display much more homogeneous spectra.

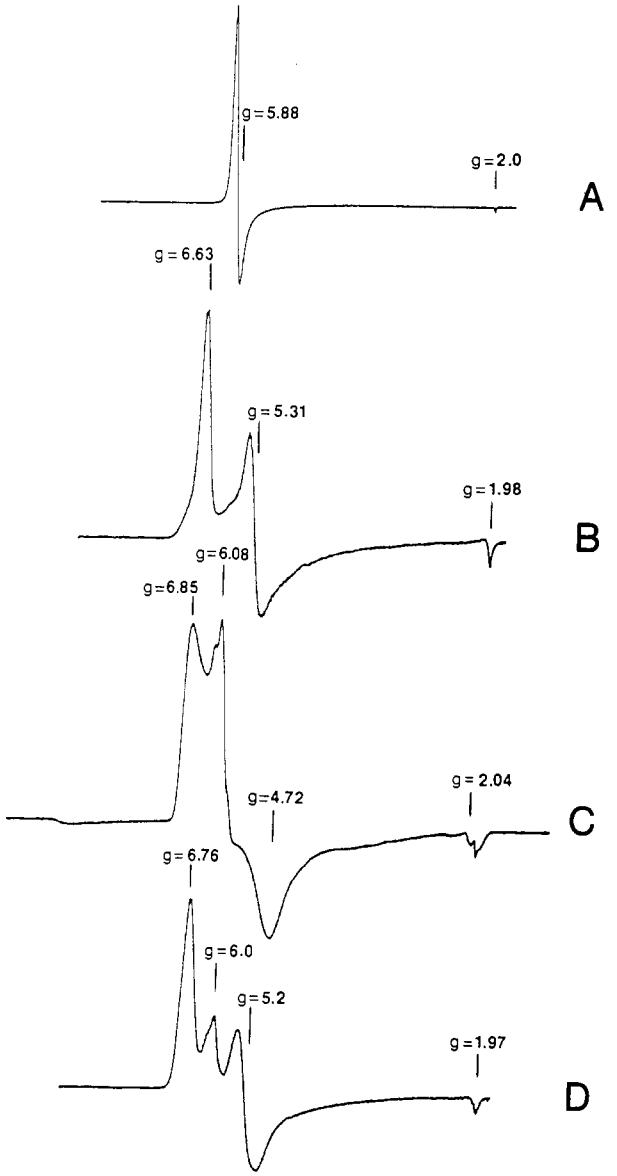

FIGURE 2: Electron paramagnetic resonance spectra of wild-type and mutant myoglobins at 7.3 K: (A) wild-type Mb, in 0.1 M potassium phosphate (pH 7.0), microwave frequency 9.431 GHz; (B) His(E7)Tyr Mb, in 0.1 M potassium phosphate (pH 7.0), microwave frequency 9.427 GHz; (C) His(F8)Tyr Mb, in 0.1 M potassium phosphate (pH 9.0), microwave frequency 9.4341 GHz; (D) Val(E11)Glu Mb, in 0.1 M potassium phosphate (pH 7.0), microwave frequency 9.4361 GHz.

Table II: Percent Rhombicity[a]

protein	% rhombicity
ferrihemoglobin A	0.8
ferrimyoglobin	0.8
Hb M Iwate [His(αF8)Tyr]	2.4
Hb M Boston [His(αE7)Tyr]	3.7
Hb M Hyde Park [His(βF8)Tyr]	3.9
bacterial catalase	6.5
cyt-*c*–imidazole complex	6.8
bovine liver catalase (type I)	7.5
erythrocyte catalase	7.5
Hb M Saskatoon [His(βE7)Tyr]	8.1
His(E7)Tyr Mb	8.19
Val(E11)Glu Mb	10.8
Hb M Milwaukee [Val(βE11)Glu]	11.3
bovine liver catalase (type II)	11.7
cytochrome P-450$_{cam}$	26.0

[a] Percent rhombicity is defined as $R = (\Delta g/16) \times 100$ (Peisach et al., 1971), where Δg is the absolute difference in g values between the two components near $g = 6$. Table modified from Palmer (1979).

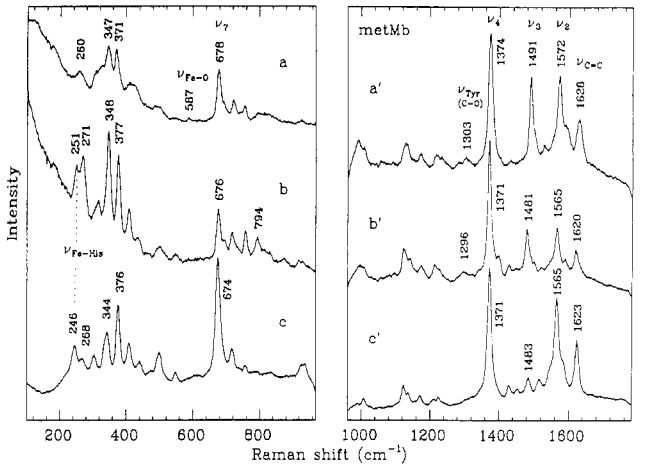

FIGURE 3: Resonance Raman spectra of the His(F8)Tyr Mb in 0.1 M potassium phosphate (pH 9.0) (a and a′), His(E7)Tyr Mb in 0.1 M potassium phosphate (pH 7.0) (b and b′), and native met-Mb in 0.1 M potassium phosphate (pH 7.0) (c and c′). The laser excitation wavelength was 416 nm with optical multichannel detection (spectrograph band-pass 7.5 cm^{-1}, 2400 groove/mm grating). The total integration and averaging time is 10 min for the mutant samples and 20 and 60 min for the high- and low-frequency native sample, respectively. The power at the sample is 14 mW for the mutant samples and 3 mW for the native material. Typical protein concentrations are 30–100 μM.

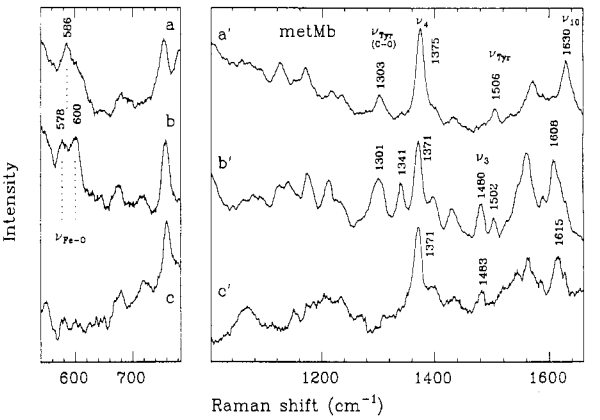

FIGURE 4: Raman spectra of the His(F8)Tyr Mb in 0.1 M potassium phosphate (pH 9.0) (a and a′), His(E7)Tyr Mb in 0.1 M potassium phosphate (pH 7.0) (b and b′), and native met-Mb in 0.1 M potassium phosphate (pH 7.0) (c and c′) taken with 488-nm laser excitation. The spectrograph band-pass is 15 cm^{-1}, and 1200 groove/mm gratings are used. The total integration and averaging time is 20–50 min for each spectrum. The sample concentrations are 560 μM (a and a′), 295 μM (b and b′), and 870 μM (c and c′). The laser power is increased to 50–200 mW due to the weak resonance conditions.

Resonance Raman Spectroscopy. Figures 3 and 4 present the resonance Raman spectra of native met-Mb and the oxidized mutant proteins with tyrosine replacement at positions F8 and E7. The laser excitation in Figure 3 is 416 nm so that direct resonance with the Soret band is achieved. In Figure 4 the laser excitation is moved to 488 nm in order to explore the iron–tyrosine charge-transfer resonance (Nagai et al., 1983; Pyrz et al., 1985). The high-frequency region of Figure 3 reveals bands characteristic of the oxidation (ν_4) and spin and coordination (ν_2, ν_3) states of the heme iron atom (Spiro, 1983). All the oxidized samples are found to be in the ferric high-spin state. As exhibited by the ν_3 peak at 1481 cm^{-1}, the iron atom is six-coordinate in the native and His(E7)Tyr Mb proteins, where weakly bound water and tyrosine E7 (vide infra) are coordinated as sixth ligands, respectively. In contrast, the His(F8)Tyr Mb mutant shows a significant upshift of the ν_3 and ν_2 marker bands (Figure 3a′), to 1491 and 1572 cm^{-1},

Table III: Resonance Raman Frequencies of Mutant and Native Sperm Whale Mb and Human Hb[a]

			Fe^{3+} 488-nm Excitation					
mode	His(F8)Tyr Mb	His(E7)Tyr Mb	native Mb	Hb M Saskatoon	Hb M Boston	Hb M Hyde Park	Hb M Iwate	Hb A
ν_{10}	1630	1608	1615	1607	1628	1628	1628	1611
ν_{Tyr}	1506	1502	absent	1504	1505	1502	1504	absent
ν_3	absent	1480	1483	1479	1490	1489	absent	1478
ν_4	1375	1371	1371	1372	1372	1372	1372	1372
$\nu_{Tyr(C-O)}$	1303	1301	absent	1300	1278	1300	1308	absent
$\nu_{Fe-O(phenolate)}$	586	578/600	absent	578	603	588	588	absent

	Fe^{3+} 416-nm Excitation			
mode	His(F8)Tyr Mb	His(E7)Tyr Mb	Val(E11)Glu Mb	native Mb
$\nu_{C=C}$	1628	1620	1623	1623
ν_2	1572	1565	1565	1565
ν_3	1491	1481	1483	1483
ν_4	1374	1371	1372	1371
$\nu_{Tyr(C-O)}$	1303	1296	absent	absent
ν_7	678	676	675	674
ν_{Fe-His}	see text	251	251	246

	Fe^{2+} 430-nm Excitation			
mode	His(F8)Tyr Mb	His(E7)Tyr Mb	Val(E11)Glu Mb	native Mb
$\nu_{C=C}$	1621	1618	1618	1619
ν_2	1561	1564	1563	1564
ν_3	1471	1472	1470	1472
ν_4	1358	1356	1355	1357
ν_7	675	674	674	675
ν_{Fe-His}	absent	222	220	221

	Fe^{2+}–CO 420-nm Excitation			
mode	His(F8)Tyr Mb	His(E7)Tyr Mb	Val(E11)Glu Mb	native Mb
$\nu_{C=C}$	1622	1621	1621	1621
ν_2	1585	1587	1589	1588
ν_3	1501	1501	1501	1501
ν_4	1374	1374	1374	1374
ν_7	677	676	676	676
ν_{Fe-CO}	499	494	508	508
ν_{255}	absent	255	255	255

[a] Raman mode assignments and frequencies for Hb M mutants and Hb A from Nagai et al. (1989).

respectively, which reflects the smaller core size associated with five-coordinate, high-spin iron. Of interest is the relative absence of the 1491-cm^{-1} mode (ν_3) of the His(F8)Tyr Mb at 488-nm excitation (Figure 4a′) versus its presence with Soret excitation (Figure 3a′). This coordination state marker was also absent for Hb M Iwate, while the intensity of this mode was greatly reduced in Hb M Hyde Park with 488-nm excitation wavelength (Nagai et al., 1989; Table III). The depolarized ν_{10} mode observed with 488-nm excitation is upshifted in the His(F8)Tyr Mb mutant spectrum (Figure 4a′), which is also consistent with the five-coordinate assignment (Nagai et al., 1989). Also worth noting is the relative enhancement of the 794 and 1341-cm^{-1} modes in His(E7)Tyr Mb (Figures 3b and 4b′) and the reduced intensity of the ν_7 mode at approximately 675 cm^{-1} in both tyrosine mutant samples. These observations indicate significant differences in the Raman excitation profiles of these modes and reflect subtle alterations in the electronic structure and electron–nuclear coupling of these systems.

The presence of the iron–tyrosine linkage in both the F8 and E7 ferric Mb tyrosine mutants is demonstrated by the enhancement of the tyrosine-specific ν_{Fe-O} (ca. 590 cm^{-1}) and internal tyrosine modes (ca. 1300 and 1500 cm^{-1}) in Figures 3 and 4 (Nagai et al., 1989). These modes are barely observable in the Soret excited spectra (Figure 3) but show a dramatic increase in relative intensity upon movement of the laser excitation to 488 nm (Figure 4). This is consistent with the charge-transfer enhancement mechanism proposed previously (Nagai et al., 1983). The ν_{Fe-O} mode exhibited by the His(E7)Tyr Mb mutant has an apparent doublet structure with frequencies at 600 and 578 cm^{-1}, while the His(F8)Tyr Mb exhibits one ν_{Fe-O} mode at 586 cm^{-1} (Figure 4a,b). A flexibility of the Fe–O linkage in the Hb mutants is indicated by the broad line widths and differing peak positions observed for ν_{Fe-O} (Nagai et al., 1989). The distinct peaks at 578 and 600 cm^{-1} in the six-coordinate His(E7)Tyr Mb may indicate the presence of two separate tyrosine–iron conformations having different bond strengths that correlate with Hb M Saskatoon (ν_{Fe-O} = 578 cm^{-1}) and Hb M Boston (ν_{Fe-O} = 603 cm^{-1}) (Table III; see Discussion). In comparison, the His(F8)Tyr Mb mutant shows a single value for ν_{Fe-O} (586 cm^{-1}), which is similar to that observed for Hb M Hyde Park and Hb M Iwate (Nagai et al., 1989).

A band at approximately 250 cm^{-1} that is associated with the ν_{Fe-His} and/or the pyrrole tilting vibration in native met-Mb (Teraoka & Kitagawa, 1981; Choi & Spiro, 1983) is observed in Figure 3. This band is also observed in the His(E7)Tyr Mb (Figure 3b), but its relative intensity is altered with respect to the other low-frequency bands, particularly the 271-cm^{-1} mode. The absence of the 250-cm^{-1} mode in the His(F8)Tyr Mb mutant spectrum (Figure 3a) indicates that the proximal ligand–iron linkage is strongly perturbed, as expected. The observation of iron–tyrosine-specific modes (Figure 4a), along with the five-coordinate assignment, suggests that iron coordination by the distal histidine is minimal at room temperature. On the other hand, the weak band at 260 cm^{-1} in Figure 3a could conceivably indicate the presence of such an E7 histidine–iron complex in dynamic equilibrium with the F8 tyrosine ligated iron (vide infra). In an attempt to probe whether the weak 260-cm^{-1} mode is due to an iron–histidine ligand, a pH titration was undertaken. Between pH 9 and pH 5.5 no alteration of the 260-cm^{-1} mode was observed (data not shown);

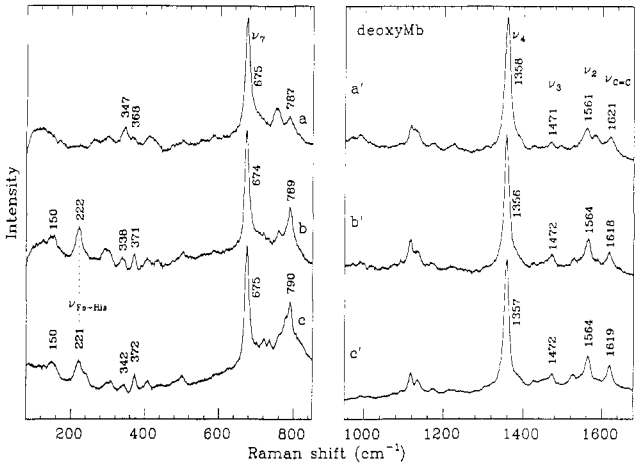

FIGURE 5: Same as Figure 3 except for deoxy-Mb. The excitation wavelength is 430 nm. The total integration and averaging time is 2 min for the mutant samples and 23 and 38 min for the high- and low-frequency region of the native sample, respectively. The power is 40 mW for the mutant samples and 15 mW for the native material. Note the striking absence of the 221- and 150-cm^{-1} modes in the spectrum of the His(F8)Tyr Mb mutant (a).

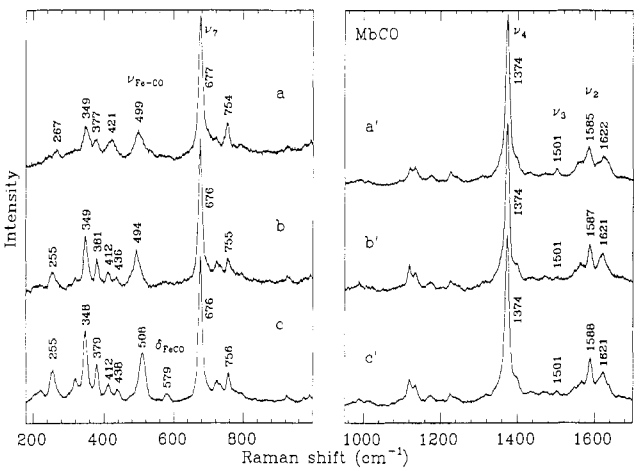

FIGURE 6: Same as Figure 3 except for MbCO and spinning-cell geometry. The excitation wavelength is 420 nm. The total integration and averaging time is 5 min for the mutant samples and 10 min for the native material. The power at the sample is 3–4 mW, and the beam was defocused.

below pH 5.5 this mutant was unstable. The absence of intensity changes at 260 cm^{-1} at low pH, therefore, makes an iron–histidine assignment unlikely (see Discussion).

Figure 5 displays the Soret excited Raman spectra of the reduced myoglobin proteins. The frequencies ν_2 (ca. 1564 cm^{-1}), ν_3 (ca. 1472 cm^{-1}), and ν_4 (ca. 1357 cm^{-1}) are consistent with a five-coordinate high-spin ferrous heme in all samples. In the low-frequency region, the 220-cm^{-1} ν_{Fe-His} mode (Kitagawa et al., 1979; Choi & Spiro, 1983; Argade et al., 1984) and the associated 150- and 240-cm^{-1} modes of native Mb have disappeared in His(F8)Tyr deoxy-Mb while these modes are present in His(E7)Tyr deoxy-Mb (Figure 5a,b).

Figure 6 presents the Raman spectra of the CO-bound samples. The ν_{Fe-CO} vibration is observed near 500 cm^{-1} in native Mb, His(E7)Tyr Mb, and His(F8)Tyr Mb, as expected for histidine-coordinated heme proteins (Yu & Kerr, 1989), although the intensity of the Fe–CO mode is reduced in both mutant samples. The differences found in the His(F8)Tyr Mb mutant spectrum involve the absence of the 255-cm^{-1} mode and an appearance of a weak spectral feature at 267 cm^{-1}. The doublet at approximately 412–438 cm^{-1} also merges into a single broad line at 421 cm^{-1}, as is also seen in the oxidized

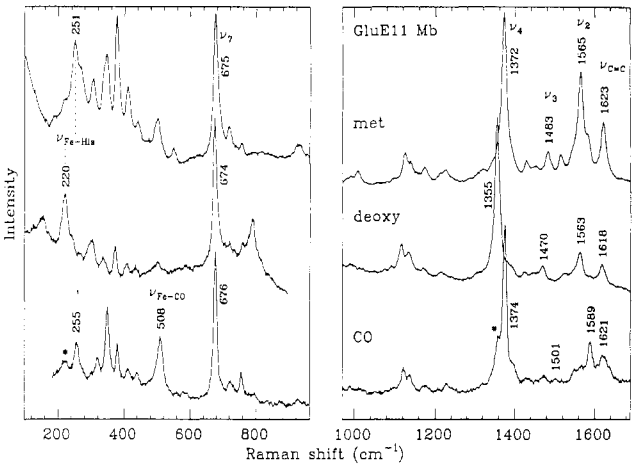

FIGURE 7: Resonance Raman spectra of the Val(E11)Glu Mb mutant in 20 mM Tris-HCl (pH 8.4) and 1 mM EDTA, in the met (a and a′), deoxy (b and b′), and CO-bound (c and c′) forms. The laser excitation is 416, 430, and 420 nm, respectively, for the three samples. The power is 14 and 30 mW for the met and deoxy samples and is reduced to 2 mW (defocused beam) for the MbCO spectrum. The asterisk (*) indicates that, even at these reduced powers, some photolyzed material is present. This most likely reflects a decrease in the CO affinity for this mutant relative to that of native Mb.

and deoxy species of this mutant.

Figure 7 presents the Raman spectra for the Val(E11)Glu Mb mutant. Here we note that the Raman spectra of the oxidized, deoxy, and CO-bound forms in both the high- and low-frequency regions are nearly identical with those of the native species. The ν_{C-O} mode is found at 508 cm^{-1} in the Val(E11)Glu MbCO mutant, as is observed in the native MbCO protein, indicating that the polar glutamic acid residue at position E11 is not directly perturbing the CO-bound heme environment. However, increased laser photolysis of the CO complex of Val(E11)Glu Mb is observed by the presence of residual deoxy species in Figure 7c [denoted by an asterisk (*)] even at drastically reduced laser power. This suggests that the CO affinity for this mutant is decreased relative to that of native Mb.

DISCUSSION

In this paper, we report the combination of UV–visible, electron paramagnetic, and resonance Raman spectroscopies to assess the structural and electronic properties of the heme environment of three mutant Mb proteins: His(E7)Tyr Mb, His(F8)Tyr Mb, and Val(E11)Glu Mb. EPR methodologies for ferric heme proteins are quite sensitive to symmetry changes at the metal site due to changes in the protein structure. Departure from tetragonality reflects the direct effect of the protein environment on the heme iron. Resonance Raman can be used to assess the spin and ligation states of the heme, the status of the iron–proximal axial ligand bond, and the identity of the axial ligands. Since the functional differences in heme proteins may be correlated with the nature of the axial ligands, it is of great interest to determine the precise metal–ligand stretching modes.

Nagai and co-workers assigned the iron–tyrosine mode of naturally occurring Hb M mutants with tyrosine substitution, using excitation in the charge-transfer absorption band (Nagai et al., 1983). More recently, all four Hb M mutants with tyrosine replacements exhibited the fingerprint bands for iron–tyrosinate proteins (Que, 1988) in addition to the usual resonance Raman bands of an iron porphyrin (Nagai et al., 1989). Also worth noting are the Raman spectra of bovine liver catalase (Chuang et al., 1988) and fungal and bacterial

catalases (Sharma et al., 1989). These spectra exhibit the presence of a high-spin, ferric heme iron in these tyrosine-coordinated heme proteins. Additionally, weak vibrational modes indicative of coordinated tyrosine were observed for these catalases upon maximum enhancement with visible excitation (Chuang et al., 1988; Sharma et al., 1989).

His(E7)Tyr Mb is analogous to the Hb M mutants M Saskatoon [His(βE7)Tyr] and M Boston [His(αE7)Tyr]. The heme iron of the abnormal subunit of Hb M Boston is five-coordinate with the distal tyrosine liganded and the iron–proximal histidine bond broken (Pulsinelli et al., 1973; Nagai et al., 1983). In contrast, the abnormal β chains of Hb M Saskatoon exhibited a Raman spectral pattern of a six-coordinate heme iron ligated to tyrosine E7 and histidine F8 (Nagai et al., 1989). The EPR spectra of His(E7)Tyr Mb and Hb M Saskatoon exhibit many similarities with a high-spin rhombic split observed for both proteins, as is also observed for bovine liver catalase (Table II). In contrast, Hb M Boston displays a much lower rhombicity.

Resonance Raman spectra in Figure 3 verify that the ferric heme iron of His(E7)Tyr Mb is primarily six-coordinate, high-spin, and ligated to both the distal tyrosine and the proximal histidine. The iron–tyrosinate mode is verified by a doublet observed at 578 and 600 cm^{-1} with excitation at 488 nm (Figure 4b), while a weakening of the mode at 251 cm^{-1} is seen with Soret excitation (Figure 3b). The fact that the ν_{Fe-O} modes parallel the frequencies found for the six-coordinate Hb M Saskatoon (ν_{Fe-O} = 578 cm^{-1}) and the five-coordinate Hb M Boston (ν_{Fe-O} = 603 cm^{-1}) (Nagai et al., 1989; Table III) indicates that two well-defined tyrosine E7 binding geometries are possible in the mutant Mb. One possibility is that the histidine F8 ligand in Mb is strong enough to maintain its bond in both geometries so that the iron is found in a six-coordinate high-spin configuration for this His(E7)Tyr Mb mutant. An alternative possibility is a trans-ligand effect that involves the presence of the His F8 ligand (ν_{Fe-O} = 578 cm^{-1}) or its absence (ν_{Fe-O} = 600 cm^{-1}). This would provide a simple explanation for the equivalence of the ν_{Fe-O} frequencies. However, this would also require a significant population of five-coordinate species, which is not obvious in Figure 3b′. Nevertheless, an anonomous reviewer suggested that the shoulder at ca. 1491 cm^{-1} in the spectrum of Figure 3b′ could be interpreted as up to a 25% five-coordinate population. Such an assignment would strongly favor the latter possibility. Since the majority of the population of His(E7)Tyr Mb is clearly six-coordinate, we conclude that it resembles HbM Saskatoon much more than HbM Boston, although a minority population of five-coordinate, tyrosine-bound heme with ν_{Fe-O} = 600 cm^{-1} cannot be ruled out. Thus, it seems that two specific tyrosine binding geometries in His(E7)Tyr Mb must be primarily responsible for the observed frequencies. His(E7)Tyr deoxy-Mb is a five-coordinate, high-spin ferrous heme with the iron coordinated to the proximal histidine as indicated by the presence of a 220-cm^{-1} mode (ν_{Fe-His}) (Figure 5b). Thus the loss of the tyrosine ligand upon reduction of the iron is confirmed. This Mb mutant binds CO stably, whereas addition of O_2 results in rapid heme iron oxidation (Springer et al., 1989).

His(F8)Tyr Mb has a mutation analogous to that of Hb M Iwate [His(αF8)Tyr] and Hb M Hyde Park [His(βF8)Tyr]. Resonance Raman studies of these Hb mutants indicate that the abnormal subunit of both these Hb proteins is five-coordinate and high-spin with tyrosine F8 providing the ligation to the ferric heme iron (Nagai et al., 1989). This correlates with the Raman data of our analogous His(F8)Tyr Mb mutant, which suggest that this protein is homogeneously five-coordinate in the ferric state with only the tyrosine F8 residue liganded to the heme iron. The spectra shown in Figure 3 illustrate a tentative confirmation for the assignment of ν_{Fe-His} at ca. 250 cm^{-1} in the oxidized state (Teraoka & Kitagawa, 1981). The absence of both the 270- and 250-cm^{-1} modes for His(F8)Tyr Mb (Figure 3a) suggests that the coupling of both modes to the Soret band is associated with the proximal histidine which is removed by this mutation. However, these spectra alone do not rule out the possibility of a protein population of mixed ligation states in dynamic equilibrium between a tyrosine F8 liganded form and a second histidine E7 liganded state, with the 260-cm^{-1} spectral feature (Figure 3a) indicative of an iron–His(E7) bond. This 260-cm^{-1} frequency is quite high for Mb iron–imidazole (Teraoka & Kitagawa, 1980, 1981). However, ferric HRP–fluoride exhibits an iron–histidine mode at 267 cm^{-1} while native HRP exhibits a signal at 274 cm^{-1} (Teraoka & Kitagawa, 1981). The pH titrations of this Mb mutant revealed a fixed intensity of the 260-cm^{-1} mode down to pH 5.5 where protonation of the tyrosine F8 residue would be expected (Nagai et al., 1989) to increase the population of the iron-His(E7) complex. Thus, the identity of the 260-cm^{-1} mode remains unassigned. Nevertheless, in a frozen matrix a potentially mixed population in the ferric state of His(F8)Tyr Mb is suggested by the EPR parameters of this mutant, which reveal multiple g values. These EPR results differ from those of the analogous Hb mutants, Hb M Iwate and Hb M Hyde Park, which exhibit a homogeneous population with nearly tetragonal symmetry (Hayashi et al., 1969). In order to account for the mixed population observed at low temperatures, Raman spectroscopy was carried out at 200 K; however, we were unable to observe the oxidized species of this His(F8)Tyr Mb mutant due to facile photoreduction in the frozen state. Therefore, the conversion of the heme from a homogeneous to a mixed ligation state upon freezing could not be confirmed, and definitive assignment of the ligands to His(F8))Tyr Mb in the frozen matrix could not be made.

His(F8)Tyr deoxy-Mb is predominantly five-coordinate, high-spin (Figure 5a′). In the ferrous state, a definitive confirmation of the iron–His(F8) mode frequency is determined since the 220-cm^{-1} mode seen in the native protein, and thought to be the ν_{Fe-His} frequency (Teraoka & Kitagawa, 1981; Choi & Spiro, 1983), is absent in the His(F8)Tyr Mb mutant (Figure 5a). Thus the controversy surrounding the assignment of ν_{Fe-His} (Kitagawa et al., 1979; Nagai et al., 1980; Desbois et al., 1979; Desbois & Lutz, 1981; Argade et al., 1984) is quite clearly resolved by this spectrum. Moreover, it seems that both the 150- and 240-cm^{-1} modes must involve motions associated with the presence of the proximal histidine. This suggests that mixing of the iron–histidine stretching mode with the pyrrole tilting modes is likely (Argade et al., 1984). Thus, the absence of any frequency near 220 cm^{-1} for this mutant suggests that histidine E7 is not coordinated to the heme but rather that the proximal tyrosine F8 or another amino acid or solvent is the ligand to the ferrous iron.

The CO complex of His(F8)Tyr Mb exhibits a ν_{Fe-CO} vibration near 500 cm^{-1} which is typical for histidine-coordinated heme proteins (Yu & Kerr, 1989). In addition, this mutant exhibits a MbCO optical spectrum nearly identical with that of native sperm whale Mb (Table I), also suggestive of a histidine ligation. The possibility of histidine ligation seems reasonable on the basis of the optical absorption and EPR spectroscopies of the CO and NO complexes of Hb M Iwate (Peisach & Gersonde, 1977; Nagai et al., 1979). Both groups report the potential for ligand binding to the proximal side of the heme with HisE7 liganded to the ferrous heme iron.

However, the formation of a new ligand binding pocket on the proximal side of the heme should result in a rather drastic protein rearrangement leading to dramatically altered resonance Raman modes. As spectra a and c of Figure 6 depict for His(F8)Tyr MbCO and native MbCO, respectively, no great alterations in Raman lines are evident. No tyrosine–Fe–CO system has been studied to date, which would provide a model for assignment of such a ν_{Fe-CO} frequency. On the basis of our data, it is impossible to unequivocally confirm the axial ligand to the iron in either the deoxy or CO-bound species. A solvent water molecule or another amino acid is an alternative possibility for the fifth ligand. In addition, there is a disappearance of the 255-cm^{-1} mode in the CO-bound His(F8)Tyr Mb (Figure 6) compared to wild-type MbCO, with an appearance of a 267-cm^{-1} mode. This suggests that the 255-cm^{-1} mode is somehow associated with the presence of His(F8) in the CO-bound complex. Careful studies of this region of the spectrum along with isotopic labeling studies involving the iron and nitrogen atoms have not been reported. The assignment of the ca. 250-cm^{-1} mode to the pyrrole tilt (Choi & Spiro, 1983) is difficult to reconcile with the systematic disappearance of this mode in both the oxidized and CO-bound states when tyrosine F8 is ligated (Figures 3 and 6).

Val(E11)Glu Mb has a mutation analogous to that of Hb M Milwaukee [Val(βE11)Glu]. The X-ray crystallographic structure for ferric Hb M Milwaukee indicates a six-coordinate, high-spin protein ligated to the proximal histidine His(F8) and the distal pocket glutamate Glu(E11) (Perutz et al., 1972). We suggest that Val(E11)Glu Mb exhibits the same axial ligand arrangement as Hb M Milwaukee. The EPR spectra of these two proteins are nearly identical (Figure 2, Table II). In addition, the Raman marker frequencies suggest Val(E11)Glu Mb is six-coordinate and high-spin with the iron–proximal histidine bond intact as assigned by the 251-cm^{-1} mode (Figure 7a). We were unable to distinguish between water and a carboxylate bound to the iron in the sixth coordination position of the oxidized form of native Mb and the Val(E11)Glu Mb mutant. Since a carboxylate group is a weak ligand, as is water, the similar Raman spectra observed for these two proteins are consistent. These similar Raman spectral patterns were also observed for the β subunit of Hb M Milwaukee and met-Hb A (Nagai et al., 1983). In the deoxy state of Val(E11)Glu Mb, the Raman spectra indicate a five-coordinate high-spin protein with the iron–histidine bond intact, suggesting the proposed carboxylate ligand is lost upon reduction of the iron (Figure 7b). Boxer and co-workers have also constructed a Val(E11)Glu mutant using the human Mb gene and reported ligation properties similar to those of Hb M Milwaukee (Varadarajan et al., 1989a,b). Since the sperm whale and human Mb proteins are very closely related, it follows that many of the conclusions reached concerning altered axial ligation properties for these proteins are consistent. For example, both proteins exhibit the optical absorption spectral shift of ca. 635 to ca. 620 nm for the ligand to metal charge-transfer band of the ferric protein upon substitution of valine E11 with glutamic acid. This spectral feature is also seen in Hb M Milwaukee, thus lending credence to the proposal that all three proteins exhibit similar ligation properties.

Site-directed mutagenesis has been used extensively to probe protein structure–function relationships. As can be observed in this paper, site-directed mutagenesis also provides a specific means by which new spectroscopic (EPR and resonance Raman) characteristics may be identified or suspected frequencies confirmed. For example, we have used the assigned Raman frequencies for ν_{Fe-His} in the oxidized (ca. 250 cm^{-1}) and reduced states (ca. 220 cm^{-1}), as well as the $\nu_{Fe-O(phenolate)}$ frequencies (ca. 590 cm^{-1}) seen in the oxidized states, in order to draw detailed conclusions regarding the ligation states of the various synthetic sperm whale Mb mutants. In addition, when histidine F8 is replaced by tyrosine, we have observed the absence of those modes which are associated with the histidine–heme vibrations. Thus, site-directed mutagenesis can be used as a technique for vibrational assignment in systems with complex spectra.

ACKNOWLEDGMENTS

We thank Jean H. Lewis for her help in preparing the manuscript.

Registry No. L-His, 71-00-1; L-Val, 72-18-4; L-Tyr, 60-18-4; L-Glu, 56-86-0; Fe, 7439-89-6; heme, 14875-96-8.

REFERENCES

Argade, P. V., Sassaroli, M., Rousseau, D. L., Inubushi, T., Ikeda-Saito, M., & Lapidot, A. (1984) *J. Am. Chem. Soc. 106*, 6593.

Choi, S., & Spiro, T. G. (1983) *J. Am. Chem. Soc. 105*, 3683.

Chuang, W.-J., Johnson, S., & Van Wart, H. E. (1988) *J. Inorg. Biochem. 34*, 201.

Desbois, A., & Lutz, M. (1981) *Biochim. Biophys. Acta. 671*, 168.

Desbois, A., Lutz, M., & Banerjee, R. (1979) *Biochemistry 18*, 1510.

Dickerson, R. E., & Geis, I. (1983) in *Hemoglobin: Structure, Function, Evolution, and Pathology* (Hagopian, P., Ed.) p 32, Benjamin/Cummings, Menlo Park, CA.

Gaber, B. P., Miskowski, V., & Spiro, T. G. (1974) *J. Am. Chem. Soc. 96*, 6868.

Greer, J. (1971) *J. Mol. Biol. 59*, 107.

Hattori, M., & Sakaki, Y. (1986) *Anal. Biochem. 152*, 232.

Hayashi, A., Suzuki, T., Imai, K., Morimoto, H., & Watari, H. (1969) *Biochim. Biophys. Acta 194*, 6.

Kitagawa, T., Nagai, K., & Tsubaki, M. (1979) *FEBS Lett. 104*, 376.

Maniatis, T., Fitsch, E. F., & Sambrook, J. (1982) in *Molecular Cloning: A Laboratory Manual*, Cold Spring Harbor Laboratory, Cold Spring Harbor, NY.

Morikis, D., Champion, P. M., Springer, B. A., & Sligar, S. G. (1989) *Biochemistry 28*, 4791.

Morse, P. (187) *Biophys. J. 51*, 440a.

Nagai, K., Hori, H., Morimoto, H., Hayashi, A., & Taketa, F. (1979) *Biochemistry 18*, 1304.

Nagai, K., Kitagawa, T., & Morimoto, H. (1980) *J. Mol. Biol. 136*, 271.

Nagai, K., Kagimoto, T., Hayashi, A., Taketa, F., & Kitagawa, T. (1983) *Biochemistry 22*, 1305.

Nagai, M., & Yoneyama, Y. (1983) *J. Biol. Chem. 258*, 14379.

Nagai, M., Yoneyama, Y., & Kitagawa, T. (1989) *Biochemistry 28*, 2418.

Palmer, G. (1979) in *The Porphyrins* (Dolphin, D., Ed.) Vol. IV, p 328, Academic Press, New York.

Peisach, J., & Gersonde, K. (1977) *Biochemistry 16*, 2539.

Peisach, J., Blumberg, W. E., Ogawa, S., Rachmilewitz, E. A., & Oltzik, R. (1971) *J. Biol. Chem. 246*, 3342.

Perutz, M. F. (1970) *Nature (London) 228*, 726.

Perutz, M. F. (1987) in *The Molecular Basis of Blood Diseases* (Stamatoyannopoulos, Nienhuis, Leder, & Majerus, Eds.) pp 127–178, W. B. Saunders, Philadelphia.

Perutz, M. F., Pulsinelli, P. D., & Ranney, H. M. (1972) *Nature (London), New Biol. 237*, 259.

Pulsinelli, P. D., Perutz, M. F., & Nagel, R. L. (1973) *Proc. Natl. Acad. Sci. U.S.A. 70*, 3870.
Pyrz, J. W., Roe, A. L., Stern, L. J., & Que, L., Jr. (1985) *J. Am. Chem. Soc. 107*, 614.
Que, L., Jr. (1988) in *Biological Applications of Raman Spectroscopy* (Spiro, T. G., Ed.) Vol. 3, p 491, Wiley, New York.
Sharma, K. D., Andersson, L. A., Loehr, T. M., Terner, J., & Goff, H. M. (1989) *J. Biol. Chem. 264*, 12772.
Shimizu, T., Hirano, K., Takahashi, M., Hatano, M., & Fujii-Kuriyama, Y. (1988) *Biochemistry 27*, 4138.
Sligar, S. G., Egeberg, K. D., Sage, J. T., Morikis, D., & Champion, P. M. (1987) *J. Am. Chem. Soc. 109*, 7896.
Spiro, T. G. (1983) in *Iron Porphyrins* (Lever, A. B. P., & Gray, H. B., Eds.) Vol. 2, p 89, Addison-Wesley, Reading, MA.
Springer, B. A., & Sligar, S. G. (1987) *Proc. Natl. Acad. Sci. U.S.A. 84*, 8961.
Springer, B. A., Egeberg, K. D., Sligar, S. G., Rohlfs, R. J., Mathews, A. J., & Olson, J. S. (1989) *J. Biol. Chem. 264*, 3057.
Srajer, V., Reinisch, L., & Champion, P. M. (1988) *J. Am. Chem. Soc. 110*, 6656.
Stayton, P. S., Atkins, W. M., Springer, B. A., & Sligar, S. G. (1989) *Met. Ions Biol. Syst. 25*, 461.
Teraoka, J., & Kitagawa, T. (1980) *J. Phys. Chem. 84*, 1928.
Teraoka, J., & Kitagawa, T. (1981) *J. Biol. Chem. 256*, 3969.
Unger, B. P. (1988) Ph.D. Thesis, Department of Biochemistry, University of Illinois, Urbana–Champaign.
Varadarajan, R., Zewert, T. E., Gray, H. B., & Boxer, S. G. (1989a) *Science 243*, 69.
Varadarajan, R., Lambright, D. G., & Boxer, S. G. (1989b) *Biochemistry 28*, 3771.
Yu, N.-T. & Kerr, E. A. (1989) in *Biological Applications of Raman Spectroscopy* (Spiro, T. G., Ed.) Vol. 3, p 39, Wiley, New York.

Circular Dichroism Studies of the HIV-1 Rev Protein and Its Specific RNA Binding Site†

Thomas J. Daly,‡ James R. Rusche,‡ Theodore E. Maione,‡ and Alan D. Frankel*,§
Repligen Corporation, One Kendall Square, Building 700, Cambridge, Massachusetts 02139, and Whitehead Institute for Biomedical Research, Nine Cambridge Center, Cambridge, Massachusetts 02142
Received May 7, 1990; Revised Manuscript Received August 1, 1990

ABSTRACT: The circular dichroism (CD) spectrum of the Rev protein from HIV-1 indicates that Rev contains about 50% α helix and 25% β sheet at 5 °C in potassium phosphate buffer, pH 3, and 300 mM KF. The spectrum is independent of protein concentration over a 20-fold range. At neutral pH, Rev is relatively insoluble but can be brought into solution by binding to its specific RNA binding site, the Rev-responsive element (RRE), at a Rev:RNA ratio of about 3:1. Nonspecific binding to tRNA does not solubilize Rev. As judged by difference CD spectra, the conformation of Rev when bound to the RRE at neutral pH is similar to the conformation of unbound Rev at pH 3, although changes in the RNA may also contribute to the difference spectrum. Indeed, some difference is observed near 260 nm, consistent with a conformational change of the RRE upon Rev binding. Rev alone at pH 3 shows irreversible aggregation as the temperature is raised, while Rev bound to the RRE at neutral pH shows a reversible transition with a T_m of 68 °C.

Human immunodeficiency virus (HIV) encodes several regulatory proteins in addition to the Gag, Pol, and Env gene products encoded by most retroviruses. At least two of these regulatory proteins, Tat and Rev, are essential for viral replication (Fisher et al., 1986; Dayton et al., 1986; Sodroski et al., 1986; Terwilliger et al., 1988) and therefore are potential targets for anti-HIV drugs. Tat is a transactivator that increases expression of all viral genes and seems to function at both the transcriptional and posttranscriptional levels [see Cullen and Greene (1989) for a review]. Rev, a small protein of 13 000 daltons, appears to function posttranscriptionally (Malim et al., 1989; Hammarskjold et al., 1989) and is localized to the nucleus and nucleolus (Cullen et al., 1988; Perkins et al., 1989). In the absence of Rev, viral transcripts are fully spliced, resulting in production of both Rev and Tat proteins (Knight et al., 1987). Rev then increases the levels of incompletely spliced mRNAs that are transported to the cytoplasm, shifting viral protein synthesis toward production of the structural proteins (Sodroski et al., 1986; Feinberg et al., 1986; Knight et al., 1987; Sadaie et al., 1988; Malim et al., 1988; Hammarskjold et al., 1989). It has not yet been determined whether Rev acts by suppressing splicing (Feinberg et al., 1986; Emerman et al., 1989), by causing release of mRNAs from the spliceosome (Chang & Sharp, 1989), or by facilitating mRNA transport (Malim et al., 1989a; Felber et al., 1989; Hammarskjold et al., 1989).

The site of action for Rev is a highly conserved sequence located within the *env* gene, called the Rev-responsive element (RRE) (Malim et al., 1989a; Hadzopoulou-Cladaras et al., 1989; Rosen et al., 1988). This region forms a highly structured RNA element which must be maintained in the proper orientation to remain Rev-responsive (Dayton et al., 1989; Olsen et al., 1990; Malim et al., 1989a). Deletions within the RRE have defined at least one domain, the "hammerhead", as being necessary for Rev function (Dayton et al., 1989; Olson et al., 1990; Malim et al., 1990). Recently, several studies have shown that purified Rev binds with high affinity and

† This research was supported by the Lucille P. Markey Charitable Trust (A.D.F.), by NIH National Institute of Allergy and Infectious Diseases Grant AI29135 (A.D.F.), and by Sandoz Research Institute, Sandoz Ltd.
* To whom correspondence should be addressed.
‡ Repligen Corporation.
§ Whitehead Institute for Biomedical Research.

0006-2960/90/0429-9791$02.50/0